Jurnal Presipitasi
Media Komunikasi dan Pengembangan Teknik Lingkungan
e-ISSN: 2550-0023
Vol 23, No 2, 2026, 473-487
Article available at homepage presipitasi

Original Research Article

Effects of Steam Pretreatment and Delignification Time on Balsa Wood Polyvinyl Alcohol Composites

Sena Maulana[1,5*], Fajar Aditya Julyatmojo[1], David Raja Endar Ambarita[1], Laras Widi Setia Ningrum[1], Jabosar Ronggur Hamonangan Panjaitan[2], Muhammad Iqbal Maulana[3], Sarah Augustina[3], Muhammad Aizat Abdul Ghani[4]

[1] Department of Forestry Engineering, Institut Teknologi Sumatera (ITERA), Jalan Terusan Ryacudu, Way Hui, Kecamatan Jati Agung, Lampung Selatan, Lampung, Indonesia 35365

[2] Department of Chemical Engineering, Institut Teknologi Sumatera (ITERA), Jalan Terusan Ryacudu, Way Hui, Kecamatan Jati Agung, Lampung Selatan, Lampung, Indonesia 35365

[3] Research Center for Biomass and Bioproducts, National Research and Innovation Agency, Jalan Raya Jakarta-Bogor KM 46, Cibinong, Bogor, Jawa Barat 16911

[4] Faculty of Tropical Forestry, Universiti Malaysia Sabah, Jalan UMS, 88400, Kinabalu, Sabah, Malaysia

[5] Green and Sustainable Materials Society, Jalan Terusan Ryacudu, Way HuiK, Jati Agung, Lampung Selatan, Lampung, Indonesia 35365

* Corresponding Author, email: sena.maulana@rh.itera.ac.id

Abstract

The effect of controlled steam pretreatment on polyvinyl alcohol/balsa wood composites was investigated. Controlled steam was applied prior to subsequent sodium chlorite-acetic acid delignification of balsa wood and its impregnation with polyvinyl acetate (PVA). Low-density balsa veneers were either not subjected to steam or were steamed at 126 °C for 1 h. Wood delignification was carried out in a 1% solution of sodium chlorite-acetic acid at 80 °C for 45, 90, or 180 min. The samples were further bleached in a 3% hydrogen peroxide solution and vacuum-impregnated with 5% PVA. The Wood-PVA system was monitored using color, tensile, FTIR, and X-ray diffraction analyses. The steam-pretreated and delignified for 90 min sample (90S) exhibited the best characteristics, showing a tensile strength of 3.39 MPa and Young's modulus of 112.36 MPa. The obtained data indicated continuous removal of lignin and hemicellulose, much stronger PVA-cellulose interactions, and preservation of cellulose in its native cellulose I state without a significant decrease in crystallinity. The proposed treatment represents a reproducible way to convert balsa wood into a stiff, formaldehyde-free, and low-density composite material available for implementation in modern building technologies.

Keywords: Balsa wood; delignification; polyvinyl alcohol; steam pretreatment; tensile properties; x-ray diffraction

1. Introduction

The construction sector is under increasing pressure to reduce its environmental footprint, particularly greenhouse gas emissions, and to shift towards bio-based, renewable materials. Engineered wood and wood–polymer composites are attractive in this context because they combine a renewable resource base with favorable strength-to-weight ratios and the potential for multifunctional use in green

infrastructures. Transparent and delignified wood composites have recently emerged as a prominent material class, offering combinations of mechanical performance, low density, and tunable optical or thermal properties that are difficult to achieve with glass or petrochemical polymers alone (Jele et al., 2023; Hai et al., 2025).

Transparent and delignified wood composites are generally produced via two main steps: (i) partial removal or chemical modification of lignin and chromophores to obtain a pale, nanoporous, cellulose-rich wood template, and (ii) impregnation of this delignified template with a polymer whose refractive index and functional properties are tailored to the target application (Li et al., 2016, 2017). Delignification of transparent or modified wood is often carried out using a sodium chlorite–acetic acid system, commonly referred to as the Wise method when applied in repeated stages. This approach selectively oxidizes lignin and partially removes hemicellulose while largely preserving the crystalline cellulose framework, which is critical for mechanical stiffness (Kumar et al., 2013; Li et al., 2016). Conventional Wise-type delignification is typically conducted at 60–80 °C for several hours with repeated additions of $NaClO_2$ and acetic acid, thus consuming considerable time and chemicals (Kumar et al., 2013; Sánchez-Salvador et al., 2025). Over-extended treatment can further lead to excessive hemicellulose degradation and attack on amorphous cellulose regions, resulting in embrittlement and strength loss (Minato et al. 2007; Kumar et al. 2013). From an environmental engineering standpoint, shortening the delignification time and reducing reagent consumption without compromising mechanical properties is an important goal, as it can lower the energy demand, chemical load, and associated emissions in the manufacture of wood-based composites.

Steam and hydrothermal pretreatments are well-established tools in the biorefinery and pulp sectors for overcoming the recalcitrance of lignocellulosic biomass. Steam explosion and related treatments at elevated temperatures and pressures can disrupt the lignin–hemicellulose network, induce swelling, and generate microcracks in the wood cell wall, thereby increasing permeability and facilitating subsequent chemical penetration (Ziegler-Devin et al., 2021; Kang et al., 2021). Experimental and modelling studies have shown that internal steam pressure can rupture pit membranes and create preferential pathways for mass transport, significantly enhancing gas and liquid permeability (Wang et al., 2019; Kang et al., 2021). When properly controlled, steam pretreatment can maintain cellulose crystallinity, which is essential for load-bearing applications (Fatrawana et al. 2019; Maulana et al. 2020). However, most of these studies have focused on chips, fibers, or bulk biomass for enzymatic hydrolysis, rather than veneer-scale substrates intended as templates for delignified wood and transparent or structural wood–polymer composites. Systematic investigations on the integration of a controlled steam pretreatment step directly before sodium chlorite–acetic acid delignification to shorten the reaction time, enhance lignin removal, and influence the mechanical performance of the resulting composites remain limited.

At the impregnation stage, most reported transparent wood systems rely on thermoset or thermoplastic polymers, such as epoxy resins or poly(methyl methacrylate) (PMMA). These polymers can provide high optical transmittance and good mechanical performance; however, they are largely fossil-based and are often processed using organic solvents or energy-intensive curing cycles (Li et al., 2016; Hai et al., 2025). From the perspective of environmental technology and sustainable materials, there is a growing interest in water-borne polymer systems with low toxicity and recyclability that can be integrated with delignified wood while still delivering high stiffness and structural integrity (Jele et al., 2023; Terzopoulou et al., 2025). In parallel, polyvinyl alcohol (PVA) has attracted attention as a water-soluble polymer with low volatile organic compound (VOC) emissions for wood modification systems owing to its abundant hydroxyl groups capable of forming hydrogen bonds with cellulose and its widespread use in coatings and formulations that are biodegradable or partially biodegradable (Parit et al., 2022; Cong et al., 2024). Recent studies on PVA-based transparent wood and wood–PVA composites have shown that PVA impregnation can reduce water uptake, improve dimensional stability, and provide favorable optical and mechanical properties, especially when combined with additional inorganic or organic modifiers

(Cong et al., 2024; Terzopoulou et al., 2025). Nevertheless, many transparent wood systems still depend on epoxy or PMMA, and reports that combine PVA with sodium chlorite–acetic acid delignified wood, particularly for very low-density species such as balsa, remain relatively scarce compared with the broader transparent wood literature (Jele et al., 2023; Lü et al., 2024).

Currently, transparent and delignified wood composites are most commonly prepared by sodium chlorite bleaching in an acetate buffer, followed by polymer impregnation, yielding a white, nanoporous, cellulose-rich wood template with tunable optical and mechanical properties (Li et al., 2016; Hai et al., 2025). However, this scheme is still time- and chemical-intensive and carries the risk of structural weakening due to hemicellulose and amorphous cellulose degradation. Simultaneously, steam pretreatment, which has already been established in biorefineries and pulp mills to improve permeability and reduce biomass recalcitrance, is rarely applied systematically to veneer-scale substrates for transparent wood (Ziegler-Devin et al., 2021; Maulana et al., 2021). On the polymer side, many transparent wood systems still rely on fossil-based epoxy and PMMA, whereas water-borne PVA offers a greener alternative for achieving transparency. PVA-based transparent wood has demonstrated strong optical and mechanical performance, and PVA impregnation in wood composites has reduced water absorption while moderating shrinkage behavior (Rao et al., 2019; Cong et al., 2024). The combined use of controlled steam pretreatment, sodium chlorite–acetic acid delignification, and PVA impregnation, especially for very low-density wood such as balsa, has rarely been reported and represents a key gap in the development of sustainable wood–polymer composites (Jele et al., 2023; Lü et al., 2024).

Taken together, these considerations indicate that the development of transparent wood and delignified wood composites that are genuinely environment-oriented still leaves important gaps, particularly regarding the integration of controlled steam pretreatment before sodium chlorite–acetic acid delignification on veneer-scale substrates and the use of water-borne polymers such as PVA as alternatives to fossil-based epoxy and PMMA. Therefore, this study aimed to analyze the effect of low-temperature, controlled steam pretreatment prior to balsa delignification in a sodium chlorite–acetic acid system, followed by PVA impregnation, on the resulting engineered wood properties.

2. Materials and Methods

2.1 Materials

Balsa veneer (*Ochroma pyramidale*) with nominal dimensions of 20 mm × 20 mm × 1 mm was used as the wood substrate. Sodium chlorite ($NaClO_2$, 80.00 – 83.00%, HIMEDIA) and acetic acid (CH_3COOH) were used to prepare the delignification solution. Hydrogen peroxide (H_2O_2, Emsure, 30%; Merck) was used as a bleaching agent. PVA (Mw 89,000–98,000 g/mol, ≥99% hydrolyzed; Sigma-Aldrich) was used as the impregnating polymer. Distilled or deionized water was used for solution preparation and washing purposes.

2.2 Steam Pretreatment of Balsa Veneer

Steam pretreatment was performed in an autoclave. Balsa veneers (20 × 20 × 1 mm) were placed inside the autoclave without direct contact with liquid water, so that saturated steam acted as the main heating and conditioning medium. The autoclave was operated at 126 °C for 1 h (Fatrawana et al. 2019). After the steaming period, the system was allowed to cool to approximately 60 °C before the specimens were removed. This steam pretreatment step was intended to open wood pores, partially disrupt hemicellulose–lignin linkages, and facilitate the penetration of the delignification solution in the subsequent stage. Veneers that underwent this step are hereafter referred to as steam-pretreated (S), whereas those that did not undergo this step are referred to as non-steam (NS).

2.3 Delignification Procedure

Delignification was performed using a $NaClO_2$–acetic acid system. The delignification liquor contained 1% (w/v) sodium chlorite ($NaClO_2$) and acetic acid (CH_3COOH), and the pH was adjusted to

4.6. The solution temperature was maintained at 80 °C throughout the delignification process. Both non-steam (NS) and steam-pretreated (S) veneers were immersed in a delignification solution and treated for 45, 90, or 180 min. At the end of each delignification period, the samples were removed from the solution and thoroughly rinsed with distilled water to remove the residual chemicals. The sample codes used in this study are listed in Table 1.

Table 1. Sample codes and treatment descriptions

Sample code	Description
45NS	balsa veneer, non-steam (NS), delignified for 45 min
90NS	balsa veneer, non-steam (NS), delignified for 90 min
180NS	balsa veneer, non-steam (NS), delignified for 180 min
45S	balsa veneer, steam-pretreated (S), delignified for 45 min
90S	balsa veneer, steam-pretreated (S), delignified for 90 min
180S	balsa veneer, steam-pretreated (S), delignified for 180 min

2.4 Bleaching

After delignification and water rinsing, all samples were bleached using hydrogen peroxide. Bleaching was performed in a 3% (w/v) H_2O_2 solution at ambient temperature for 1 h to minimize further cell wall degradation during delignification treatment (Pędziwiatr et al., 2018; Firmanda et al., 2026). Following bleaching, the samples were rinsed with distilled water and air-dried for 48 h before polymer impregnation.

2.5 PVA Impregnation and Drying

The PVA solution was prepared by dissolving PVA (Mw 89,000–98,000 g/mol, ≥99% hydrolyzed; Sigma-Aldrich) in water at a 5 % (w/v) concentration. The solution was heated to 90 °C and stirred for 15 min until a homogeneous solution was formed. Balsa veneers from all treatment combinations (NS and S in 45, 90, and 180 min) that had been delignified and bleached were immersed in a 5% (w/v) PVA solution and subjected to vacuum impregnation at 0.2 kPa for 15 min to promote PVA penetration into the cell lumina and cell walls. After impregnation, the specimens were removed from the solution, gently wiped to remove excess PVA from the surface, and oven-dried at 60 °C for 48 h to solidify and fix the PVA within the wood structure. The resulting materials were referred to as PVA-modified balsa composites.

2.6 Color Measurements

Color measurements were performed using a benchtop spectrophotometer calibrated against certified white and black tiles prior to each measurement session. The instrument settings were as follows: illuminant D65, 10° observer, SCI mode (specular component included), and a 6 mm aperture. For each treatment group, each specimen was measured at five randomly distributed positions on each face, avoiding visible defects. The CIELAB coordinates L*, a*, and b* were averaged for each specimen separately. The color differences were calculated using the CIE76 Formula (1).

$$\Delta E^*_{ab} = \sqrt{(\Delta L^*)^2 + (\Delta a^*)^2 + (\Delta b^*)^2} \quad (1)$$

2.7 Mechanical Testing

The mechanical properties of the PVA-modified balsa composites were evaluated under tension. The tensile strength (MPa), Young's modulus (MPa), and elongation at break (%) were determined using a tensile method adapted from ASTM D3039. The test specimens were prepared with dimensions of 5 mm × 60 mm × 1 mm. Mechanical tests were performed using an Instron 5944 universal testing machine equipped with a 500 N load cell. The crosshead speed was set to 10 mm min^{-1}, and the initial gauge length was 25 mm. All tests were conducted with the loading direction parallel to that of the wood grain.

2.8 Functional Group and Crystallinity Analysis

Fourier transform infrared (FTIR) spectroscopy was used to examine the chemical changes in the wood and wood–PVA composites. The functional groups were analyzed using a Bruker Tensor 27 instrument (Bruker, Germany) equipped with an attenuated total reflectance (ATR) probe. Spectra were collected over the range 4000–600 cm^{-1} with a spectral resolution of 4 cm^{-1}, averaging 64 scans for each sample. X-ray diffraction (XRD) was used to assess the cellulose crystallinity in the untreated balsa, 90NS, and 90S samples. Diffraction patterns were recorded over a 2θ range of 5–85° at a scanning rate of 7° min^{-1} using a Rigaku SmartLab X-ray diffractometer with Cu Kα radiation (λ = 1.5408 Å). The crystallinity index of cellulose was calculated using the Segal method (Segal et al., 1959; Augustina et al., 2025), based on the intensity difference between the (002) crystalline peak and the amorphous background, according to Formula (2). For both FTIR and XRD analyses, the specimens were ground to a particle size below 1 mm and conditioned to minimize moisture effects on the measurements.

$$Crystallinity\ Index\ (\%) = \frac{I_{002} - I_{am}}{I_{002}} \times 100 \quad (2)$$

where I_{oo2} is the maximum intensity of the 002 crystalline peak of cellulose I (2θ ≈ 22–23°), and I_{am} is the minimum intensity at approximately 2θ ≈ 18°, which represents the amorphous component.

3. Results and Discussion

3.1 Color change after delignification

Visual changes in the appearance of balsa veneer along the non-steam (NS) and steam (S) routes are shown in Figure 1 and 2, respectively, while the corresponding CIELAB color parameters are summarized in Fig. 3. The overall color difference ΔE* ranged from approximately 5.88 to 14.17 for all treatment groups, with a general tendency to increase with longer delignification times (Figure 3). The increase in both ΔE* and L* after delignification indicates that the light-absorbing components in the cell wall, particularly lignin chromophores, are progressively removed, making the wood surface appear brighter. This observation is consistent with the attenuation of the aromatic C=O and lignocellulosic carbonyl bands in the FTIR spectra discussed in Section 3.4, which indicates a reduction in the lignin and hemicellulose content (Javier-Astete et al., 2021; Jungnikl et al., 2008).

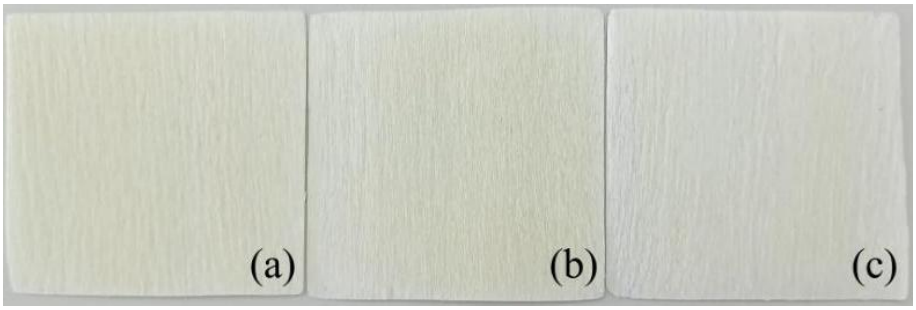

Figure 1. Visual color change of balsa veneers in the non-steam (NS) series after delignification: (a) 45NS, (b) 90NS, and (c) 180NS.

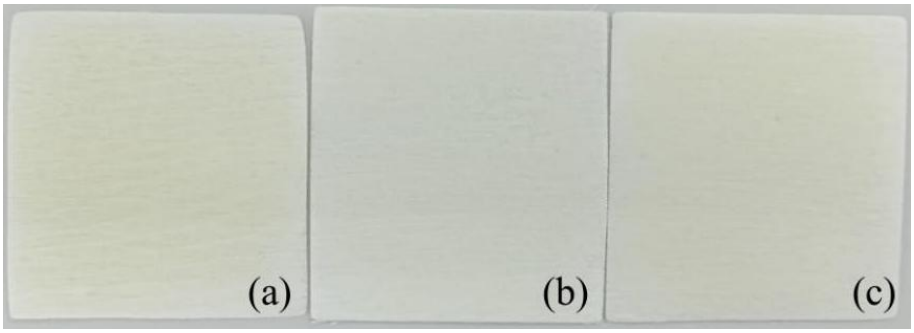

Figure 2. Visual color change of balsa veneers in the steam (S) series after delignification: (a) 45S, (b) 90S, and (c) 180S.

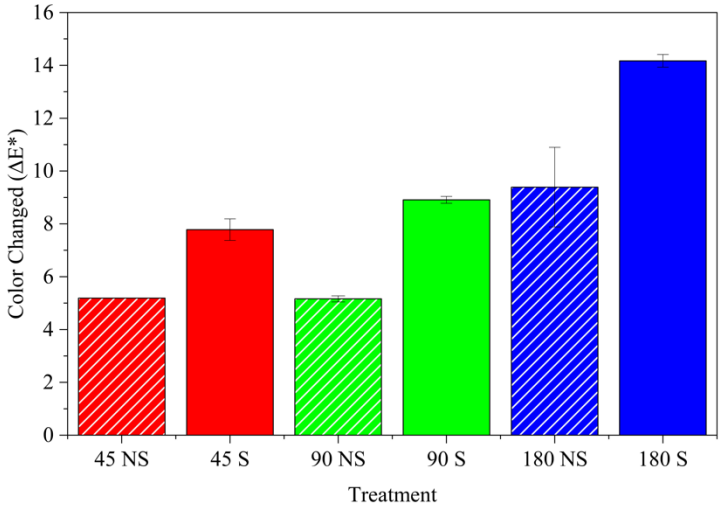

Figure 3. Lab color changes of balsa veneers in the nonsteam and steam-pretreated series after delignification.

In the 90S condition, the combination of steam pretreatment and 90 min of delignification produced the highest ΔE* and the visually brightest veneer among all treatments (Figure 2 and 3). This behavior suggests that delignification is more effective in the S series than in the NS series, consistent with reports that steam or steam explosion pretreatments can open the cell wall structure, generate microcracks, and increase the accessibility of delignifying reagents (Ziegler-Devin et al., 2021). Therefore, the color change is relevant not only from an optical perspective but also serves as an early indicator of successful lignin removal, which later influences PVA impregnation and the mechanical performance discussed in Sections 3.2 and 3.3.

3.2 Effect of Steam Treatment and Delignification Time on Tensile Strength

The tensile behavior of the PVA-modified balsa composites responded to the combination of NS/S treatment and delignification time in a nonlinear manner, as summarized in Table 2. Within the NS series, the tensile strength increased from 0.97 ± 0.08 MPa (45NS) to 1.58 ± 0.10 MPa (90NS) and then slightly decreased to 1.56 ± 0.12 MPa (180NS). In the S series, the increase was more pronounced, from 1.21 ± 0.09 MPa (45S) to 3.39 ± 0.25 MPa (90S), followed by a decrease to 1.19 ± 0.10 MPa (180S). Thus, the 90S condition more than doubled the tensile strength compared with 90NS and provided the highest value among all treatments (Table 2).

Table 2. Mechanical properties of polyvinyl alcohol-modified balsa composites under different pretreatment and delignification conditions (tensile strength, Young's modulus, and elongation at break).

Sample code	Tensile strength (MPa)	Young's modulus (MPa)	Elongation at break (%)
45NS	0.97 ± 0.08	21.73 ± 2.10	3.10 ± 0.35
90NS	1.58 ± 0.10	23.29 ± 1.90	1.70 ± 0.20
180NS	1.56 ± 0.12	15.13 ± 1.50	2.94 ± 0.30
45S	1.21 ± 0.09	39.38 ± 3.20	0.37 ± 0.05
90S	3.39 ± 0.25	112.36 ± 8.50	0.70 ± 0.08
180S	1.19 ± 0.10	31.88 ± 2.70	1.92 ± 0.22

From a mechanistic perspective, this trend is consistent with the dual role of lignin as both a diffusion barrier and structural component of the cell wall. Partial delignification at 90 min likely removes sufficient lignin and hemicellulose to open the pore network and expose cellulose fibrils, increasing the internal surface area available for hydrogen bonding with PVA and improving load transfer while avoiding excessive damage to the cellulose framework (Kumar et al., 2021; Terzopoulou et al., 2025). This interpretation is supported by the FTIR results for the delignified veneers in Section 3.4, where the decrease in C=O and aromatic bands indicates a reduction in lignin and hemicellulose together with an increase in the cellulose O–H band (Javier-Astete et al., 2021; Jungnikl et al., 2008).

Previous studies have reported similar behavior, namely that moderate delignification of wood or bamboo can enhance tensile strength, whereas overly aggressive delignification leads to strength loss due to damage to the cell wall network and embrittlement (Wu et al., 2019; Wu et al., 2020; Hai et al., 2025; Jele et al., 2023). This pattern helps to explain the reduction in tensile strength at 180NS and 180S, where prolonged oxidative treatment likely removes not only lignin and hemicellulose but also part of the amorphous cellulose, so that the load-bearing network becomes more fragile, while XRD still indicates preservation of the main cellulose I structure after delignification (Section 3.6).

Steam pretreatment prior to delignification further amplified these effects. Subcritical steam is known to cause cell wall swelling, middle lamella softening, microcrack formation, and increased reagent accessibility in lignocellulosic matrices (Ziegler-Devin et al., 2021). Under the 90S condition, the combination of steam and intermediate delignification time probably resulted in a more uniform delignification profile across the veneer thickness. This situation facilitates a more homogeneous PVA infiltration and the formation of a cellulose–PVA composite network that is more efficient in carrying tensile loads. The FTIR spectra after PVA impregnation (Section 3.5) are consistent with this observation, as the 90S composite shows the strongest enhancement of the O–H and C–O bands, which is indicative of more extensive PVA–cellulose interactions (Potdar et al., 2023; Žigon et al., 2025).

The role of PVA as a cavity-filling matrix is also closely linked to delignification degree. Studies on PVA-based wood composites have shown that more open pore structures and better interfacial compatibility result in greater gains in tensile strength and toughness (Rao et al., 2019; Cong et al., 2024). In the 90S composite, a relatively intact yet more porous cellulose network, supported by the preserved cellulose I structure observed in the XRD results (Section 3.6), seems to provide a favorable balance between the intrinsic load-bearing capacity of the cellulose skeleton and the contribution of PVA as a stress-bridging and crack-damping phase. In contrast, at 180S, the more severely damaged cell wall cannot fully exploit PVA infiltration, so the tensile strength decreases even though delignification has proceeded further.

Taken together, these observations indicate that 90S represents a realistic operating window for environmentally oriented applications in the tropics. This condition combines efficient delignification, good PVA infiltration, and preservation of mechanical integrity in a low-density wood–PVA composite system.

3.3 Effect on Stiffness (Young's modulus) and Ductility (elongation at break)

As shown in Table 2, the evolution of Young's modulus follows a pattern similar to that of the tensile strength. In the NS series, the modulus increased slightly from 21.73 ± 2.10 MPa (45NS) to 23.29 ± 1.90 MPa (90NS) and then decreased to 15.13 ± 1.50 MPa (180NS). In the S series, the modulus was much higher, with 39.38 ± 3.20 MPa (45S), a sharp increase to 112.36 ± 8.50 MPa (90S), and a decrease to 31.88 ± 2.70 MPa (180S). This indicates that 90S increases stiffness by almost a factor of five compared with 90NS and by approximately a factor of three compared with 45S. This behavior is consistent with reports on densified wood after partial delignification, where the modulus of elasticity can increase by 10 to 800% relative to the original wood when the degree of delignification and densification falls within an optimum range (Alqrinawi et al., 2024).

The increase in Young's modulus at 90NS and, more prominently, at 90S can be linked to two mutually reinforcing factors. First, sufficient removal of lignin and hemicellulose while retaining a continuous cellulose framework, as indicated by the attenuation of the lignin/hemicellulose C=O bands in the FTIR spectra (Section 3.4). Second, a dense hydrogen-bonding network between PVA and cellulose within the cell wall is reflected in the strengthening of the O–H and C–O bands after PVA impregnation (Section 3.5) (Potdar et al., 2023; Bantu and Kumar, 2025; Žigon et al., 2025; Cong et al., 2024). Similar mechanisms have been reported for transparent and delignified wood that is subsequently densified or impregnated with polymers, where partial delignification, preservation of the cellulose framework, and polymer infiltration together lead to substantial gains in Young's modulus and strength (Hai et al., 2025; Jele et al., 2023; Jakob and Gindl-Altmutter, 2023).

The decline in the modulus at 180NS and 180S suggests that further extending delignification begins to compromise the integrity of the cellulose network, while XRD indicates that the cellulose I structure can remain preserved after delignification and that the crystallinity change is relatively small (Section 3.6). These findings indicate that the crystallinity index alone is insufficient to describe the microstructural state. Local damage, microcrack formation, and loss of continuity in the cellulose network caused by overly severe treatment can reduce the effective stiffness, although the nominal crystalline fraction changes only slightly (Park et al. 2010; Salem et al. 2023).

The elongation at break data complement this picture from the ductility standpoint. In the NS series, the elongation at break decreased from 3.10 ± 0.35% (45NS) to 1.70 ± 0.20% (90NS) and then increased again to 2.94 ± 0.30% (180NS). In the S series, the values were lower overall, namely 0.37 ± 0.05% (45S), 0.70 ± 0.08% (90S), and 1.92 ± 0.22% (180S). In general, S samples were stiffer and more brittle than NS samples at the same delignification time, particularly for 45S and 90S (Table 2). This trend is consistent with studies on transparent and densified wood, which often report that gains in modulus and tensile strength due to delignification and polymer impregnation are accompanied by reduced elongation at break and a shift towards more brittle fracture behavior (Rao et al., 2019; Xia et al., 2021; Hai et al., 2025).

In this context, the 90S offers a clear compromise. The Young's modulus and tensile strength were substantially increased, while the elongation at break of 0.70 ± 0.08% remained within an acceptable range for panel or core applications, where stiffness and strength are prioritized over large deformation capacity.

3.4 FTIR Analysis of Delignified Balsa

The FTIR spectra of delignified balsa in the NS and S series (Figure 4) exhibit a broad O–H stretching band at approximately 3335 cm^{-1}, C=O bands at approximately 1733 and 1646 cm^{-1}, and a C–O band at approximately 1037 cm^{-1}, which are characteristic of lignocellulosic systems (cellulose–hemicellulose–lignin) (Javier-Astete et al., 2021). The increase in the O–H band intensity at 45 and 90 min (45NS/45S and 90NS/90S) indicates that more cellulose hydroxyl groups are exposed as lignin and hemicellulose are removed. This trend is consistent with the color lightening and higher ΔE* values

discussed in Section 3.1, since the loss of lignin chromophores is also reflected in the reduction of carbonyl and aromatic bands in the FTIR spectra (Javier-Astete et al., 2021; Jungnikl et al., 2008).

A slight decrease in the O–H intensity at 180 min suggests the onset of modification or partial degradation of cellulose chains under prolonged oxidative conditions, which is in agreement with in situ FTIR studies of oxidative aging in cellulose (Łojewska et al., 2005). The gradual weakening of the C=O bands at approximately 1733 and 1646 cm^{-1}, which are associated with carbonyl groups in hemicellulose and lignin, reflects the progressive removal of non-cellulosic components. This behavior is in line with FTIR studies on extracted or delignified wood and biomass, where the reduction of carbonyl and aromatic bands is commonly used as an indicator of lignin and hemicellulose removal and enrichment of the holocellulose fraction (Javier-Astete et al. 2021; Jungnikl et al. 2008).

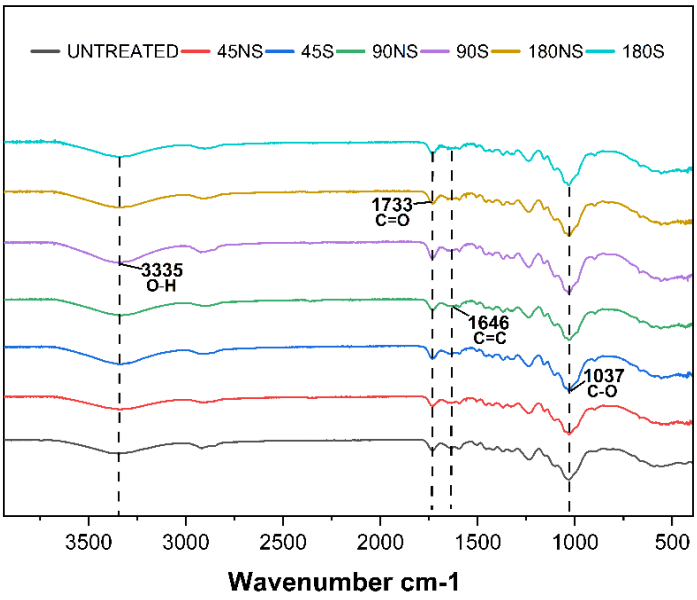

Figure 4. Fourier transform infrared spectra of delignified balsa veneers in the non-steam and steam-pretreated series, showing changes in functional groups as a function of delignification time.

Changes in the intensity and shape of the C–O band near 1037 cm^{-1} (C–O–C and C–O in polysaccharides) indicate a reorganization of the holocellulose environment, with cellulose contributing more strongly relative to hemicellulose after delignification. When NS and S samples are compared at 90 min, the steam-pretreated veneer (90S) shows a more pronounced weakening of the C=O bands and a clearer strengthening of the O–H band than 90NS. This pattern suggests more effective delignification and a "cleaner" cellulose fraction in 90S. This is also consistent with reports on steam and steam explosion pretreatments, where pressurized steam and rapid depressurization promote cell wall swelling, microcrack formation, and improved accessibility of reagents to the lignocellulosic matrix (Ziegler-Devin et al., 2021).

At 180 min, subtle changes in the O–H and C–O bands in both the NS and S series imply that the treatment severity started to exceed the optimum. Under these conditions, parts of the cellulose phase are likely modified and become more susceptible to the formation of new carbonyl groups, as observed in FTIR-based studies of cellulose degradation (Lojewska et al., 2005). This interpretation is consistent with the decrease in tensile strength and modulus at 180NS and 180S (Sections 3.2 and 3.3), which shows that excessively aggressive delignification no longer benefits mechanical performance.

3.5 FTIR Analysis of PVA-Modified Balsa

The FTIR spectra of the PVA-modified balsa composites (Figure 5) displayed the combined signatures of cellulose and PVA. The broad O–H stretching band at approximately 3335 cm^{-1} became wider and more intense after PVA impregnation, reflecting overlapping contributions from the PVA and

cellulose hydroxyl groups and a denser network of intermolecular hydrogen bonds. The increase in the intensity of the C–O/C–O–C band in the 1030–1050 cm^{-1} region is also consistent with the introduction of additional C–O bonds from the PVA chains within the cell wall network. This spectral evolution agrees with reports on PVA–starch–rice straw composites and other PVA–polysaccharide films, where a broad O–H band at 3300–3400 cm^{-1} and C–O–C bands in the 995–1123 cm^{-1} region are key indicators of hydrogen-bonded networks between PVA and lignocellulosic phases (Potdar et al., 2023; Bantu and Kumar, 2025).

When 90NS and 90S composites were compared, the S sample showed the most pronounced enhancement of the O–H and C–O bands. This finding indicates a higher PVA fraction and stronger interactions with the cellulose framework in 90S, which is consistent with the higher tensile strength and Young's modulus reported in Table 2. In studies of wood coatings based on PVA reinforced with CNF, similar changes in the O–H band near 3300 cm^{-1} and the C–O band around 1070 cm^{-1} have been linked to the formation of a dense hydrogen-bonding network among PVA, CNF, and wood surfaces, which directly contributes to improved surface hardness and dimensional stability (Žigon et al., 2025).

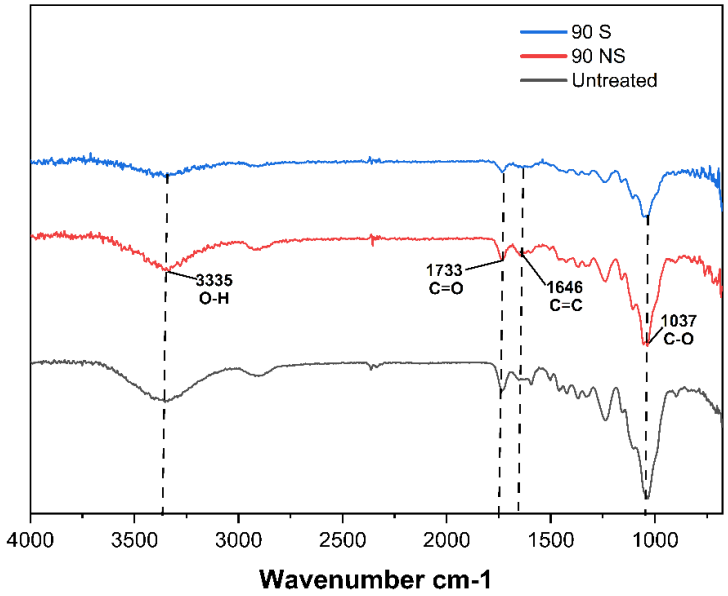

Figure 5. Fourier-transform infrared spectra of delignified balsa veneers before and after polyvinyl alcohol impregnation in the non-steam and steam-pretreated series.

Other modified wood systems, such as delignified poplar impregnated with PVA–silica, have also employed FTIR to verify the successful integration of PVA into the cell wall and track changes in lignocellulosic functional group ratios after delignification (Cong et al., 2024). The agreement between the enhancement of the O–H and C–O bands in the 90S composite and the improved mechanical properties supports the interpretation that the combination of steam pretreatment, 90 min delignification, and PVA impregnation results in a cellulose–PVA network with more continuous hydrogen bonding and more efficient stress transfer.

3.6 XRD Analysis and Crystallinity Changes

The XRD patterns of untreated, NS-delignified, and S-delignified balsa (Figure 6) show that the main diffraction peak around $2\theta \approx 22.4–22.5°$, assigned to the (002) plane of cellulose I, was preserved across all treatments. This observation indicates that the cellulose I crystal structure was not significantly altered by the processing sequence. The crystallinity index decreased from 64.07% in untreated balsa to 61.24% in NS-delignified balsa and 61.50% in S-delignified balsa (Table 3). Although the change is modest, this trend suggests that delignification affects the relative crystalline fraction to a limited extent while preserving the native cellulose I structure.

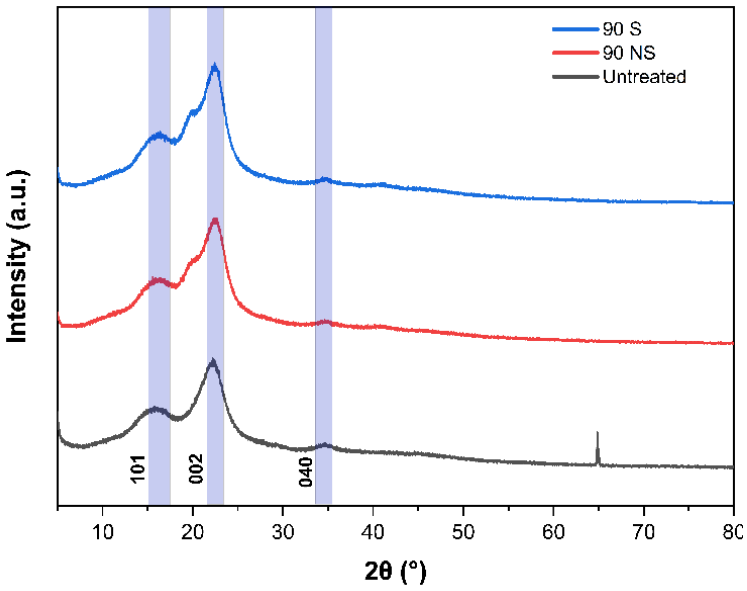

Figure 6. X-ray diffraction diffractograms of the untreated balsa, 90NS, and 90S samples, showing the main cellulose I (002) reflection and changes in the crystallinity index.

Table 3. X-ray diffraction peak positions (2θ) and crystallinity indices of cellulose for untreated balsa, 90NS, and 90S samples

Treatment	2θ (°)	Miller index	Crystallinity (%)
Untreated balsa	22.36	002	64.07
NS-delignified balsa	22.53	002	61.24
S-delignified balsa	22.53	002	61.50

From a mechanical viewpoint, the preservation of the cellulose I structure generally supports stiffness and dimensional stability in engineered wood. This is consistent with the high Young's modulus observed for the 90S composite (Section 3.3). The crystallinity values obtained here indicate that steam pretreatment and delignification can remove amorphous components while maintaining the main cellulose framework, so that the load-bearing structure remains effective.

In this context, the small difference between the NS-delignified and S-delignified balsa, combined with the decline in mechanical properties (Sections 3.2 and 3.3), suggests that an overly severe treatment starts to damage the cellulose network, even though the cellulose I crystal structure is still preserved. This conclusion is consistent with methodological studies on crystallinity, which emphasize that absolute crystallinity values are strongly dependent on the calculation method and are not always sensitive to microstructural damage (Park et al., 2010; Salem et al., 2023). Therefore, the values reported here should be interpreted as relative numbers within a single dataset rather than directly compared with other systems that use different analytical procedures. Nevertheless, the preservation of the main cellulose I peak across all treatments indicates that delignification and steam pretreatment did not destroy the native cellulose crystal structure.

3.7 Overall Implications for Environmentally Friendly Wood–PVA Composites

Overall, the color, mechanical, FTIR, and XRD data indicate 90S as the most balanced condition for balsa–PVA composites. Steam pretreatment combined with 90 min of delignification resulted in the highest tensile strength and modulus, clear color lightening, and preservation of the cellulose framework, while avoiding the severe cellulose damage indicated at 180NS and 180S. Short delignification (45 min) does not sufficiently open the pore network and cellulose–PVA interface, whereas long delignification

(180 min) over-attacks the cell wall, resulting in a decline in mechanical properties. This intermediate optimum is consistent with reports that partial delignification provides the best compromise between cellulose skeleton purification and mechanical integrity (Kumar et al., 2021; Terzopoulou et al., 2025).

From a design perspective, the key message is that the performance is governed by the engineering of the wood hierarchy. The 90S condition produces a cellulose framework that is adequately depleted of lignin and hemicellulose, preserves the native cellulose I structure, and allows more homogeneous PVA impregnation, as confirmed by FTIR and XRD, which in turn explains the strong gain in stiffness and strength with acceptable ductility. In terms of sustainability, the balsa–PVA route combines a fast-growing wood resource with a water-based matrix and avoids formaldehyde resins, placing it in the emerging family of formaldehyde-free wood composites, especially if future work moves toward bio-based PVA or PVA–biopolymer blends (Bekhta 2023; Cong et al. 2024; Potdar et al. 2023). However, to fully support the claim of environmentally friendly performance, further studies on durability, end-of-life options, and dedicated life cycle assessment of the steam–delignification–PVA process are still required, including a comparison with other bio-based wood composite systems (Rai et al., 2022; Kivikytö-Reponen et al., 2024).

4. Conclusions

This study shows that combining steam pretreatment with $NaClO_2$–acetic acid delignification and PVA impregnation can significantly improve the performance of balsa-based composites. Steam pretreatment followed by 90 min of delignification (90S) provides the most balanced conditions, with the highest tensile strength and Young's modulus, clear color lightening, and an intact cellulose framework. Shorter delignification (45 min) does not sufficiently open the pore network and cellulose–PVA interface, whereas longer delignification (180 min) starts to damage the cell wall, resulting in a decrease in stiffness and strength. FTIR and XRD analyses confirmed that the process selectively removed amorphous lignin and hemicellulose, preserved the native cellulose I structure despite a slight decrease in crystallinity after delignification, and promoted strong PVA–cellulose interactions.

From a materials perspective, balsa–PVA processed at 90S offers a promising route toward formaldehyde-free, water-based wood composites. Further work on durability, recyclability, and life cycle assessment is still needed to quantify the environmental benefits and benchmark this system against other bio-based wood composites.

Acknowledgement

This work was supported by the Penelitian Dosen Pemula grant (1483az/IT9.2.1/PT.01.03/2025) from the Ministry of Higher Education, Science and Technology, Republic of Indonesia.

Ethics Statement

This study did not involve human participants, animals, or any sensitive data. Therefore, ethical approval was not required for this study.

CRediT Author Statement

Sena Maulana: Idea Development, Research Design, Result Verification, Data Curation, Manuscript Draft Preparation, Manuscript Review and Revision, Visualization, Supervision. **Fajar Aditya Julyatmojo**: Research Design, Program Development, Formal Analysis, Investigation, Data Curation, Manuscript Draft Preparation, Manuscript Review and Revision, Visualization. **David Raja Endar Ambarita:** Research Design, Program Development, Formal Analysis, Investigation, Data Curation, Manuscript Draft Preparation, Manuscript Review and Revision, Visualization. **Laras Widi Setia Ningrum:** Research Design, Program Development, Formal Analysis, Investigation, Data Curation, Manuscript Draft Preparation, Manuscript Review and Revision, Visualization. **Jabosar Ronggur**

Hamonangan Panjaitan: Formal Analysis, Investigation, Data Curation. **Muhammad Iqbal Maulana:** Research Design, Program Development, Formal Analysis, Investigation, Data Curation. **Sarah Augustina**: Result Verification, Formal Analysis, Data Curation, Supervision. Muhammad Aizat Abdul Ghani: Formal Analysis, Data Curation, Manuscript Draft Preparation, Manuscript Review and Revision, Visualization.

References

Alqrinawi, H., B. Ahmed, Q. Wu, H. Lin, S. Kameshwar, and M. Shayan. 2024. Effect of partial delignification and densification on chemical, morphological, and mechanical properties of wood: structural property evolution. Industrial Crops and Products 213, 118430.

Augustina, S., Dwianto, W., Bahanawan, A., Sejati, P.S., Amin, Y., Darmawan, T., Wahyudi, I., Karlinasari, L., Juliana, I., Isoda, H., Gérardin, P., Lubis, M.A.R. 2025. In-situ modification of wood polymer via impregnation with ultra-low molar ratio urea-formaldehyde resins. European Journal of Wood and Wood Products 83(39).

Bantu, T.R. and A.C. Kumar. 2025. Polyvinyl alcohol/chitosan blending films supplemented with Crotalaria pallida fibers: Preparation and characterization. RASĀYAN Journal of Chemistry 18(1), 546–555.

Bekhta, P. 2023. Recent developments in eco-friendly wood-based composites II. Polymers 15(8), 1941.

Cong, R., T. Cai, S. Ge-Zhang, H. Yang, and C. Zhang. 2024. Fabrication of PVA–silica sol wood composites via delignification and freezing pretreatment. Polymers 16(13), 1949.

Fatrawana, A., S. Maulana, D.S. Nawawi, R.K. Sari, W. Hidayat, S.H. Park, F. Febrianto, S.H. Lee, and N.H. Kim. 2019. Changes in chemical components of steam-treated betung bamboo strands and their effects on the physical and mechanical properties of bamboo-oriented strand boards. European Journal of Wood and Wood Products 77, 731–739.

Firmanda, A., R.W. Nurhayati, F. Fahma, P. Cognet, K. Namhaed, H. Hermansyah, M. Sahlan, I.M. Hidayatullah, K. Lischer, and M. Gozan. 2026. Efficient H_2O_2-system for fiber delignification-bleaching and its environmental impact. Discover Materials 6, 66.

Hai, L.V., N. Srikanth, T.D.T. Le, S.H. Park, and T.H. Kim. 2025. Transparent wood fabrication and applications: A review. Molecules 30(7), 1506.

Jakob, M. and W. Gindl-Altmutter. 2023. The effect of partial delignification on the stress–strain relationship in transverse compression. Journal of Materials Science 58, 1071–1085.

Javier-Astete, R., J. Jimenez-Davalos, and G. Zolla. 2021. Determination of hemicellulose, cellulose, holocellulose and lignin content using FTIR in *Calycophyllum spruceanum* (Benth.) K. Schum. and *Guazuma crinita* Lam. PLOS ONE 16(10), e0256559.

Jele, T.B., J. Andrew, M. John, and B. Sithole. 2023. Engineered transparent wood composites: A review. Cellulose 30, 5447–5471.

Jungnikl, K., O. Paris, P. Fratzl, and I. Burgert. 2008. The implication of chemical extraction treatments on the cell wall nanostructure of softwood. Cellulose 15(3), 407–418.

Kang, C.-W., H. Kolya, E.-S. Jang, S. Zhu, and B.-S. Choi. 2021. Steam exploded wood cell walls reveals improved gas permeability and sound absorption capability. Applied Acoustics 179, 108049.

Kivikytö-Reponen, P., S. Fortino, V. Marttila, A. Khakalo, K. Kolari, A. Puisto, D. Nuvoli, and A. Mariani. 2024. An AI-driven multiscale methodology to develop transparent wood as sustainable functional material by using the SSbD concept. Computational and Structural Biotechnology Journal 25, 205–210.

Kumar, R., F. Hu, C.A. Hubbell, A.J. Ragauskas, and C.E. Wyman. 2013. Comparison of laboratory delignification methods, their selectivity, and impacts on physiochemical characteristics of cellulosic biomass. Bioresource Technology 130, 372–381.

Kumar, A., T. Jyske, and M. Petrič. 2021. Delignified wood from understanding the hierarchically aligned cellulosic structures to creating novel functional materials: A review. Advanced Sustainable Systems 5(5), 2000251.

Li, Y., Q. Fu, S. Yu, M. Yan, and L. Berglund. 2016. Optically transparent wood from a nanoporous cellulosic template: Combining functional and structural performance. Biomacromolecules 17(4), 1358–1364.

Li, Y., Q. Fu, R. Rojas, S. Yu, M. Yan, M. Lawoko, and L. A. Berglund. 2017. Lignin-retaining transparent wood. ChemSusChem 10(17), 3445-3451.

Łojewska, J., P. Miśkowiec, T. Łojewski, and L.M. Proniewicz. 2005. Cellulose oxidative and hydrolytic degradation: In situ FTIR approach. Polymer Degradation and Stability 88(3), 512–520.

Lü, Z., Q. Gao, M. Shi, Z. Su, G. Chen, H. Qi, B. Lü, and F. Peng. 2024. Colorful room-temperature phosphorescence including white afterglow from mechanical robust transparent wood for time delay lighting. Small Structures 5, 2300567.

Maulana, M.I., M. Marwanto, M. Sena, A.T. Putri, N.O. Putri, D. Prasetia, D.S. Nawawi, S. Nikmatin, F. Febrianto, and N.-H. Kim. 2020. Pengaruh modifikasi steam dan pembilasan NaOH terhadap keasaman enam jenis bambu. Jurnal Ilmu dan Teknologi Kayu Tropis 18(1), 11–18.

Maulana, S., W. Hidayat, I. Sumardi, N.J. Wistara, M.I. Maulana, J.H. Kim, S.H. Lee, N.-H. Kim, and F. Febrianto. 2021. Properties of dual-species bamboo-oriented strand boards bonded with phenol formaldehyde adhesive under various compression ratios. BioResources 16(3), 5422–5435.

Minato, K., H. Hosoo, and S. Kawaguchi. 2007. Contribution of lignin to the reactivity of wood in chemical modifications II: Influence of delignification on reaction with vaporous formaldehyde. Journal of Wood Science 53, 255–257.

Parit, M., H. Du, X. Zhang, and Z. Jiang. 2022. Flexible, transparent, UV-protecting, and water-resistant nanocomposite films based on polyvinyl alcohol and kraft lignin-grafted cellulose nanofibers. ACS Applied Polymer Materials 4(5), 3587–3597.

Park, S., J.O. Baker, M.E. Himmel, P.A. Parilla, and D.K. Johnson. 2010. Cellulose crystallinity index: Measurement techniques and their impact on interpreting cellulase performance. Biotechnology for Biofuels 3(1), 10.

Pędziwiatr, P., F. Mikołajczyk, D. Zawadzki, K. Mikołajczyk, and A. Bedka. 2018. Decomposition of hydrogen peroxide – kinetics and review of chosen catalysts. Acta Innovations 26, 45–52.

Potdar, P.P., P. Kaur, M. Singh, M.B. Kulkarni, and S. Radhakrishnan. 2023. Structure development and properties of plasticized PVA–starch–paddy straw composites. Cellulose Chemistry and Technology 57(9–10), 1073–1085.

Rai, R., R. Ranjan, and P. Dhar. 2022. Life cycle assessment of transparent wood production using emerging technologies and strategic scale-up framework. Science of the Total Environment 846, 157301.

Rao, A.N.S., G.B. Nagarajappa, S. Nair, A.M. Chathoth, and K.K. Pandey. 2019. Flexible transparent wood prepared from poplar veneer and polyvinyl alcohol. Composites Science and Technology 182, 107719.

Salem, K.S., N.K. Kasera, M.A. Rahman, H. Jameel, Y. Habibi, S.J. Eichhorn, A.D. French, L. Pal, and L.A. Lucia. 2023. Comparison and assessment of methods for cellulose crystallinity determination. Chemical Society Reviews 52(18), 6417–6446.

Sanchez-Salvador, J.L., G. Pettersson, A. Mattsson, A. Blanco, P. Engstrand, and C. Negro. 2025. Tuning chemithermomechanical pulps to achieve sustainable packaging materials: Study of fines and lignin content. Wood Science and Technology 59, 82.

Segal, L., J.J. Creely, A.E. Martin, and C.M. Conrad. 1959. An empirical method for estimating the degree of crystallinity of native cellulose using the X-ray diffractometer. Textile Research Journal 29(10), 786–794.

Terzopoulou, P., E.C. Vouvoudi, and D.S. Achilias. 2025. Delignification as a key strategy for advanced wood-based materials: Chemistry, delignification parameters, and emerging applications. Forests 16(6), 993.

Wang, C., R. Li, C. Liu, and X. Wang. 2019. Effects of medium-low temperature hydrothermal treatment on microstructure and dimensional stability of Chinese sweetgum wood. Wood Research 64(1), 97–104.

Wu, J., Y. Wu, F. Yang, C. Tang, Q. Huang, and J. Zhang. 2019. Impact of delignification on morphological, optical and mechanical properties of transparent wood. Composites Part A: Applied Science and Manufacturing 117, 324–331.

Wu, Y., J.C. Zhou, Q.T. Huang, F. Yang, Y.J. Wang, and J. Wang. 2020. Study on the properties of partially transparent wood under different delignification processes. Polymers 12(3), 661.

Xia, Q., C. Chen, T. Li, S. He, J. Gao, X. Wang, and L. Hu. 2021. Solar-assisted fabrication of large-scale, patternable transparent wood. Science Advances 7(5), eabd7342.

Ziegler-Devin, I., L. Chrusciel, and N. Brosse. 2021. Steam explosion pretreatment of lignocellulosic biomass: A mini-review of theoretical and experimental approaches. Frontiers in Chemistry 9, 705358.

Žigon, J., I. Poljanšek, P. Oven, M. Petrič, and U. Osolnik. 2025. Application and characterization of poly(vinyl alcohol) reinforced with cellulose nanofibrils as a coating for wood. Cellulose 32, 6229–6252.